International Journal of Information, Control and Computer Sciences
ISSN: 2517-9942
Vol:9, No:8, 2015

A Four-Step Ortho-Rectification Procedure for Geo-Referencing Video Streams from a Low-Cost UAV

B. O. Olawale, C. R. Chatwin, R. C. D. Young, P. M. Birch, F. O. Faithpraise, A. O. Olukiran

***Abstract*—**In this paper, we present a four-step ortho-rectification procedure for real-time geo-referencing of video data from a low-cost UAV equipped with a multi-sensor system. The basic procedures for the real-time ortho-rectification are: (1) decompilation of the video stream into individual frames; (2) establishing the interior camera orientation parameters; (3) determining the relative orientation parameters for each video frame with respect to each other; (4) finding the absolute orientation parameters, using a self-calibration bundle and adjustment with the aid of a mathematical model. Each ortho-rectified video frame is then mosaicked together to produce a mosaic image of the test area, which is then merged with a well referenced existing digital map for the purpose of geo-referencing and aerial surveillance. A test field located in Abuja, Nigeria was used to evaluate our method. Video and telemetry data were collected for about fifteen minutes, and they were processed using the four-step ortho-rectification procedure. The results demonstrated that the geometric measurement of the control field from ortho-images is more accurate when compared with those from original perspective images when used to pin point the exact location of targets on the video imagery acquired by the UAV. The 2-D planimetric accuracy when compared with the 6 control points measured by a GPS receiver is between 3 to 5 metres.

***Keywords*—**Geo-referencing, ortho-rectification, video frame, self-calibration, UAV, target tracking.

I. Introduction

MANY Unmanned Aerial Vehicle (UAV) technologies have been developed, refined and used for military applications and in the private sector. These have led to useful applications in both the public and private sectors. Typically for all these applications, the key component is the onboard sensor systems (video camera and the GPS/INS). In the private sector, the sensors system are used for different kinds of applications, among which are homeland security [1], forestry fire monitoring [2], intelligent surveillance and target acquisition. In addition, [3] also used a low-cost UAV for real-time monitoring of buried oil pipeline right-of-way for third party incursion detection. Other researchers, such as [4]-[8] have used their UAV for different kinds of application, which present different difficulties that require customized solutions.

The flight of the low-cost UAV is generally less-stable when compared with larger fixed-wing aircraft and because it flies at low altitude (approximately 500 m), the camera frame tends to jerk continuously along the flight path. This, coupled with the disorientation caused by long viewing of the video camera, makes the analysis of data acquired by the low-cost UAV difficult. Thus, the ortho-rectification and geo-referencing of the video data could serve as an important post-processing step preceding the analysis of the UAV data. Ortho-rectification is the process of geometrically correcting an aerial image such that the scale is uniform. The ortho-image formed from the process is corrected for lens distortion, topographic relief, and camera tilt. This can be used to measure true distances, because it is represents the exact measurement of the earth surface. Ortho-rectification and geo-referencing are essential to pin point the exact location of targets in video imagery acquired at the Unmanned Aerial Vehicle (UAV) platform. This can only be achieved by comparing such video imagery with an existing digital map. However, it is only when the image is ortho-rectified with the same co-ordinate system as an existing map that such a comparison is possible. Many approaches have been presented for ortho-rectification and geo-referencing of low-cost UAVs by researchers in the past. These range from using different types of operational platforms such as satellite [9], fixed-wing aircraft [10], helicopters and UAVs; and different sensors like radar [11], visible and multi-spectral images [12]. Also, many mathematical models have been used for ranging from the simple affine transformation [13] to projective transformation [14]. Geo-referencing in general is based on direct geo-referencing using a GPS/INS system, but because of the low quality of the GPS/INS usually used for low-cost UAVs during data acquisition, the GPS/INS accuracy is very low.

In this paper, a four-step ortho-rectification procedure for geo-referencing video streams transmitted from a low-cost UAV to pin point exact location of a target on video imagery in real time is presented. The method used in this paper is based on the photogrammetry model [15] this is a form of geometry imaging system that makes use of the aerial image central perspective and the principle of collinearity. A close alternative to this photogrammetry method, are the Laser scanner and the Push-broom [16]. These two approaches were observed by [17] and it was found to be time consuming and very expensive.

II. UAV System Overview

The UAV used in the experimental work reported in this paper is the Spreading Wings S800, which is a product of Djibouti Dow Jones (DJI) Industry Ltd, as shown in Fig. 1. It is a lightweight, multi-functional hexa-rotor integrated aircraft. Table I, shows the main specification of the DJI S800. The UAV consists of integrated GPS/INS for position, altitude control and a 7.5R/C flight simulator which is used for flying the UAV from the ground control station. The UAV supports up to 50 way-points in the flight plan.

B. O. O. is with the University of Sussex, United Kingdom (e-mail: boo23@sussex.ac.uk).

Fig. 1 Spreading Wings S800 [18]

The GPS/INS has been integrated on board into the center frame. This allows raw images captured to be linked to the exact time of acquisition of images. The DJI S800 gives real-time flight data and video feeds with a 5.8G video downlink via a radio signal [18].

TABLE I
DJI SPREADING WINGS S800 SPECIFICATION [18]

Diagonal Wheelbase	800mm
Frame Arm Length	350mm
Center Frame Diameter	240mm
Bi-Pod Size	500mm(Length)×415mm(Width)×320mm(Height) width: 145mm)
Max Power	360W
Signal Frequency	30Hz – 450Hz
Total weight	2.6Kg

Tables II and III show the specification of the sensors and camera employed.

TABLE II
SENSORS SPECIFICATIONS [18]

Size	17.3 x 13 mm
Diagonal	21.64 mm
Surface Area	224.9 mm^2
Pixel Pitch	3.74 μm
Pixel Area	13.99 μm^2
Pixel Density	MP/cm^2

TABLE III
CAMERA SPECIFICATIONS [18]

Resolution	17.20 Megapixels
Sensor Size	Four Thirds (17.3 x 13 mm)
Sensor Resolution	4620 x 3474
Crop Factor	2
Video Recording	1920 x 1080p

III. DATA COLLECTION

The experiments were conducted on a calibrated control field at the federal capital territory Abuja, Nigeria. The control field coverage area is 0.11357 square kilometres (sq km). Six ground control points (GCPs) were collected using a hand held GPS receiver, and these ground control points, which are located at the corners of sidewalk and crossroad, were observed till four satellites are locked simultaneously before readings were taken. In addition to the GCPs obtained from the hand-held GPS a 2D digital map of the control field.

The aerial platform includes the UAV and the sensor systems (camera and GPS/INS system). The UAV which is equipped with an auto-pilot system, flies along the predefined control area and collects video streams of the test area, while the on board GPS/INS system simultaneously collects telemetry data of the test area. The telemetry data consists of the UAV's position and angular attitude. All data collected and their source are also summarized in Table IV.

TABLE IV
DATA COLLECTION SOURCE AND PURPOSE

Data	Purpose
Mpeg-based video stream	Captured by UAV video camera to pin point exact locations of targets.
Telemetry Data	Captured by the GPS/INS system on the UAV platform. It consists of the UAV's position and angular attitude.
GCPs	Captured by hand-held GPS receiver. It is used to measure the X and Y coordinates of the GCPs.

The video and the telemetry data were collected for approximately 15 minutes and are transmitted through a radio link of 2.4GHz to the portable PC at the ground station in real time. In order to perform a near real-time image geo-referencing of the video streams acquired by the UAV platform, it is essential to generate an ortho-image from the image sequence. Due to the limited payload weight on the UAV platform we were forced to off-load this process to the ground station (Fig. 2).

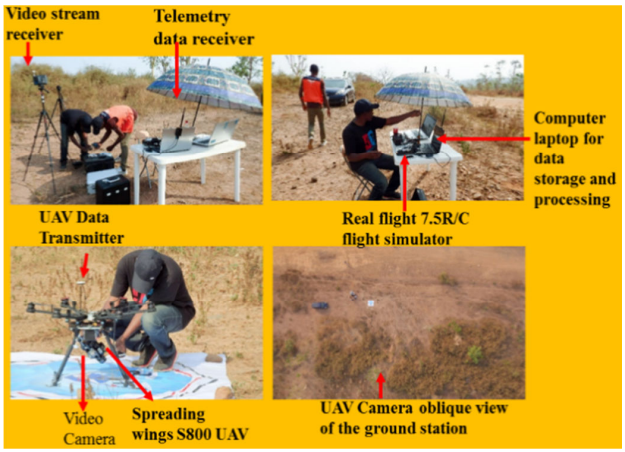

Fig. 2 Ground control Station

Since the GPS and INS are integrated into the camera on board; the received video sequence frames are time and position tagged. Fig. 3 shows the GPS flight elevation against distance covered by the UAV. The unstable lines in the graph are an indication of continuous jerking of the aircraft along the flight line. Hence, this is the cause of distortion in the captured images and the need for ortho-rectification of those images.

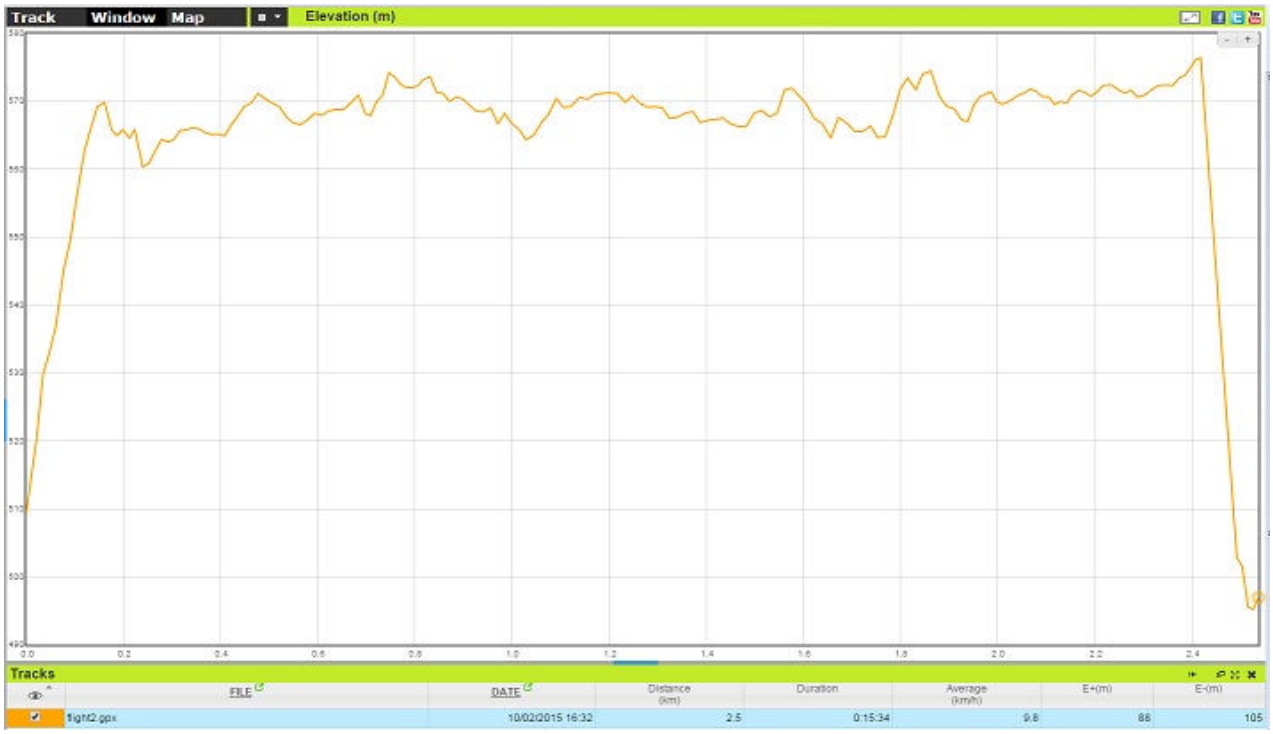

Fig. 3 GPS/INS Flight Track Log (Elevation vs. Distance)

IV. Mathematical Model for Multi-Sensor Data Fusion

The relationship between the video camera, GPS/INS and the ground points as shown in Fig. 4 is given by [19] as:

$$q_G^F = q_{GPS}^F(t) + Q_{INS}^F(t)\,[s_F * Q_C^{INS}\,(q_g^C(t) + q_{GPS}^C)] \quad (1)$$

where, q_G^F is the georeferenced 3D position vector of any point G in the image frame, $q_{GPS}^F(t)$ is a 3D vector representing the co-ordinate of the GPS antenna phase center in the mapping frame, at a particular period of time, $Q_{INS}^F(t)$ is a rotational matrix which rotates the GPS/INS sensor body frame to the given mapping frame and it consists of three attitude rotation angles (i.e. roll, pitch and yaw), these three rotational angles are concatenated into a single matrix in (2), s_F represents an image point scale factor, Q_C^{INS} is a transformation matrix called boresight matrix, it rotates the INS body frame into the c frame (i.e. offset between the image frame and the GPS/INS body frame), $q_g^C(t)$ is a 3D coordinate vector of the image point g in the image, which synchronised with the GPS periodic time (t) and q_{GPS}^C is the vector offset between the geometric centre of the GPS antenna and the camera lens centre, which is usually measured on the ground as part of the calibration process.

$$Q_{INS}^F = \begin{bmatrix} \cos\phi\cos\kappa & \cos\omega\sin\kappa + \sin\omega\sin\phi\cos\kappa & \sin\omega\sin\kappa - \cos\omega\sin\phi\cos\kappa \\ -\cos\phi\sin\kappa & \cos\omega\cos\kappa - \sin\omega\sin\phi\sin\kappa & \sin\omega\cos\kappa + \cos\omega\sin\phi\sin\kappa \\ \sin\phi & -\sin\omega\cos\phi & \cos\omega\cos\phi \end{bmatrix} \quad (2)$$

where ω, ϕ and κ represent roll, pitch, and yaw, respectively. Hence, the relationship between the two sensors and the ground point is to mathematically solve for Q_C^{Att} in the matrix equation in (1), which is usually done by a least squares adjustment with the aid of a number of well distributed GCPs.

V. Ortho-Rectification and Geo-Referencing of Video Streams

The basic steps for video imagery ortho-rectification and geo-referencing are described in the following sub-sections:

A. Decompilation of Video Stream into Individual Frames

The first step in ortho-rectification and geo-referencing video streams is the decompilation of video streams captured at the UAV platform to individual frames. There is a lot of commercial software for the decompilation of video streams into individual frames. In this paper the BPS video converter 1. 4 software is used to resample the video streams acquired at the UAV platform. Afterwards, a feature based algorithm is used for feature points extraction and image matching from the video frames. We chose feature based matching because, it is invariant to radiometric changes and it runs faster when compared with other matching techniques. Also the features used are points rather than lines. This enables us to avoid problems caused by broken lines, points are very easy to describe and are invariant to projection. Feature points are extracted and matched; they are based on a number of control parameters such as window sizes and threshold values.

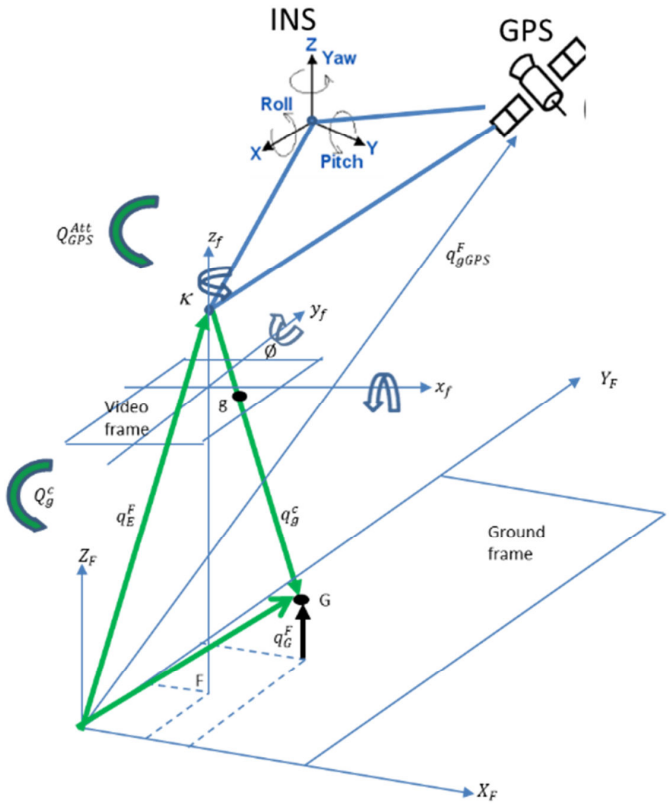

Fig. 4 Geometric Relationship between GPS/INS, Video frame and the 3D world coordinates [19]

In the Spreading Wings S800 the GPS/INS are integrated into the camera on board, this allows for each video frame to be geo-tagged (time and position tagged).

B. Finding of Interior Camera Orientation Parameter

The next step is the finding of the interior orientation of each video frame, known as camera calibration. This involves finding the focal length of the camera, principal point co-ordinates and lens distortion of each video camera frame. For the calibration of the video camera, we used a mathematical model called the Direct Linear Transform (DLT) [20]. This model is based on the principle of co-linearity (i.e. all points must be on a straight line), and it requires foreknowledge of Ground Control Points (GCPs). The DLT model can be expressed as:

$$x - \Delta x = \frac{L_1 X_G + L_2 Y_G + L_3 Z_G + L_4}{L_9 X_G + L_{10} Y_G + L_{11} Z_G + 1} \quad (3a)$$

$$y - \Delta y = \frac{L_5 X_G + L_6 Y_G + L_7 Z_G + L_8}{L_9 X_G + L_{10} Y_G + L_{11} Z_G + 1} \quad (3b)$$

where coefficients L_1 to L_{11} are the DLT parameters that reflect the co-linearity relationship between the 3D world object coordinates and the image plane (x_1, y_1); (X_G, Y_G, Z_G) are the coordinates of the ground control point G; Δx and Δy are the optical errors and can be expressed as:

$$\Delta x = \varepsilon(L_{12} r^2 + L_{13} r^4 + L_{14} r^6) + L_{15}(r^2 + 2\varepsilon^2) + L_{16}\varepsilon\eta \quad (4a)$$

$$\Delta y = \eta(L_{12} r^2 + L_{13} r^4 + L_{14} r^6) + L_{15}\eta\varepsilon + L_{16}(r^2 + 2\eta^2) \quad (4b)$$

where,

$$[\varepsilon, \eta] = [x - x_0, y - y_0] \text{ and } r^2 = \varepsilon^2 + \eta^2$$

In (4), $L_{12} - L_{14}$ represents optical distortion while $L_{15} - L_{16}$ represents de-centred distortion, as summarised in Table V.

With the use of iterative computation and the least square method, the 11 parameters can be determined. Then both the interior orientation and the angular elements of EOP can be calculated from the 11 determined parameters. The Q_C^{Att} can then be determined from:

$$Q_C^{INS}(t) = \left[Q_F^C(t) * Q_{INS}^F(t)\right]^T \quad (5)$$

where Q_C^{INS} and Q_{INS}^F are the same as (1); Q_F^C is the rotation matrix, which is a function of the three rotation angles (ω_1, ϕ_1 and κ_1) of a video frame as shown in (2).

In this step, the camera calibration process considers the

focal length and principal point coordinates only, because the IOPs and EOPs that was solved by DLT and the boresight values will be used as initial values for the final bundle adjustment model.

TABLE V
DIRECT LINEAR TRANSFORM PARAMETERS

Parameters	Remarks
$L_1 - L_{11}$	Standard DLT parameters
$L_{12} - L_{14}$	Optical distortion terms for 3^{th},5^{th} and 9^{th} order
L_{15} and L_{16}	De-centred distortion term

C. Finding the Relative Orientation

From a single image frame, which consists of two dimensional planes, we can only get two dimensional co-ordinates. In order to get three dimension views, photogrammetry uses a method similar to the principle of human vision [21]. We are able to see objects in the 3D-world in which we are in, because our two eyes are able to receive optical information as a central perspective between images captured by both eyes. The image captured by the left eye is slightly different from the image captured by the right eye. These two images are then combined in our brain to produce a spatial impression. This is the process that enables us to estimate the distance between us and an object. When this same principle is applied in photogrammetry to get the three dimensional information it is called stereoscopic viewing [22]. To illustrate stereoscopic viewing, consider the case of aerial photogrammetry in Fig. 5 where P_1 and P_2 are the camera position on the left and right respectively, C is the corresponding projection center for each camera position, the ray from the center of projection of the left camera position to the center of projection of the right camera position is called the base or baseline and Q is the image point in the 3D world scene.

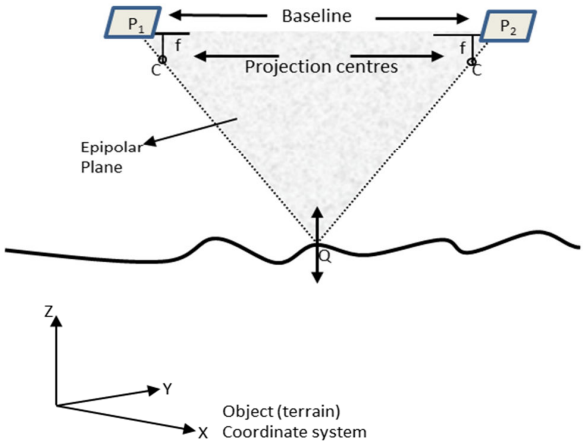

Fig. 5 Example of stereoscopic viewing with two different camera positions

If we are able to reconstruct the geometric parameters of the condition of the camera during exposure, we can then calculate the distance from the image point (Q). This can be done by setting up the two equations of the rays, and then calculating their intersection.

The process of orienting images in relation to one another, by recreating the relative position and angular attitude of images with respect to one another at the instants of exposure is called relative orientation. This is achieved in a stereoscopic pair image, by making the first image fixed and setting the Z coordinate of the first (fixed) image to its focal length, while the X and Y coordinates and the angular attitude (ω, ϕ, κ) of the fixed image are all set to zero. The X coordinate of the last image is then equal to the photo base. After the determination of the interior orientation parameters of each video frame using the DLT model as mentioned in section (V), the camera internal geometry is clearly known. Hence, the relative orientation unknown parameters can be easily solved by using pass point coordinates as observations in a least squares solution. The results obtained can then be used to attach relatively oriented image sets to each other for an entire flight strip. The entire strip is then adjusted to absolute coordinates using ground control points in a final transformation, which is discussed in the next section.

D. Finding the Absolute Orientation

The absolute orientation is the process of leveling and scaling the stereo model with respect to a reference datum using ground control points. With the relative orientation parameters computed, both the camera's interior and exterior parameters (IOPs and EOPs) are solved simultaneously by a calibration model called self-calibration bundle adjustment model. The self-calibration model used the principle of collinearity to specify the relationship between the images coordinates of points, the image space coordinate at exposure and the ground coordinates of points. The self-calibration process like the relative orientation, start with the first and second frame (a stereo pair of images) and afterwards, extended to the entire flight strip. Hence, for any ground point Q, the first video frame is given by the following mathematical model:

$$u_{q1} - u_0 + \Delta u = -f\frac{r_{11}^1(X_Q - X_{S1}) + r_{12}^1(Y_Q - Y_{S1}) + r_{13}^1(Z_Q - Z_{S1})}{r_{31}^1(X_Q - X_{S1}) + r_{32}^1(Y_Q - Y_{S1}) + r_{33}^1(Z_Q - Z_{S1}^1)} \quad (6a)$$

$$v_{q1} - v_0 + \Delta v = -f\frac{r_{11}^1(X_Q - X_{S1}) + r_{12}^1(Y_Q - Y_{S1}) + r_{13}^1(Z_Q - Z_{S1})}{r_{31}^1(X_Q - X_{S1}) + r_{32}^1(Y_Q - Y_{S1}) + r_{33}^1(Z_Q - Z_{S1}^1)} \quad (6b)$$

For the second video frame, the mathematical model is expressed as:

$$u_{q2} - u_0 + \Delta u = -f\frac{r_{11}^2(X_Q - X_{S2}) + r_{12}^2(Y_Q - Y_{S2}) + r_{13}^2(Z_Q - Z_{S2})}{r_{31}^2(X_Q - X_{S2}^2) + r_{32}^2(Y_Q - Y_{S2}) + r_{33}^2(Z_Q - Z_{S2}^1)} \quad (7a)$$

$$v_{q2} - v_0 + \Delta v = -f\frac{r_{11}^2(X_Q - X_{S2}) + r_{12}^2(Y_Q - Y_{S2}) + r_{13}^2(Z_Q - Z_{S2})}{r_{31}^2(X_Q - X_{S2}) + r_{32}^2(Y_Q - Y_{S2}) + r_{33}^2(Z_Q - Z_{S2}^1)} \quad (7b)$$

where (u_{q1}, v_{q1}) and (u_{q2}, v_{q2}) are the image coordinates of point q in the first and second video frame respectively; $(\Delta u, \Delta v)$ is as in (4); (X_Q, Y_Q, Z_Q) are object space coordinates of point Q; (X_{S1}, Y_{S1}, Z_{S1}) and (X_{S2}, Y_{S2}, Z_{S2}) are object space coordinates of the exposure station of the first and second video frame respectively; (u_0, v_0) are the principal point coordinates in the corresponding frame; f is the focal length of the camera; and the r^1 and r^2 are the elements of the three rotational angles as in (2) in the corresponding frames.

In this mathematical model, the unknown elements which consist of the camera's IOPs (u_0, v_0, f, $\Delta u, \Delta v$), and the EOPs of the first and second video frames, $(X_{S1}, Y_{S1}, Z_{S1}, \omega_1, \theta_1, \kappa_1)$ and $(X_{S2}, Y_{S2}, Z_{S2}, \omega_2, \theta_2, \kappa_2)$ respectively, can be solved by linearizing (4) and (5) using a Taylor series expansion. The linearized equation is given in matrix form as:

$$v_1 = A_1X_1 + A_2X_2 - l \quad (8)$$

where v_1 is a vector of image coordinate residuals, X_1 represents a vector of the EOPs of the two video frames, X_2 represents the vector of the camera IOPs, A_1 and A_2 are the coefficients of X_1 and X_2 respectively.

On the basis of the 6 GCPs collected as described in section (III), the co-ordinates of the image plane in the first and second video frames were measured and all the unknown parameters in (8) are solved using (5).

With the formation of ortho-image from the above process, all ortho-images (video frames) are mosaiced together to create a mosaic image covering the test area. This mosaic image is then mapped onto the digital globe containing the map of the test area and the accuracy achieved is evaluated by the use of the six ground control points obtained from the test area. The work flow of the ortho-rectification procedure is shown in Fig. 6.

VI. Experimental Results and Discussion

Figs. 7 and 8 show the result of video streams de-compilation into frames and interest points matching between two overlapping frames respectively.

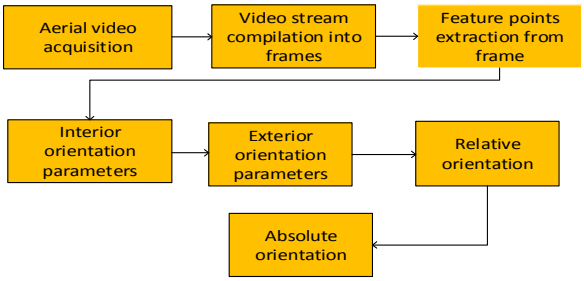

Fig. 6 Procedure workflow

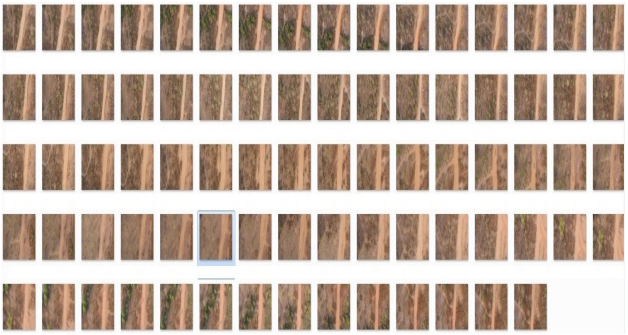

Fig. 7 Video streams decompiled into 78 frames

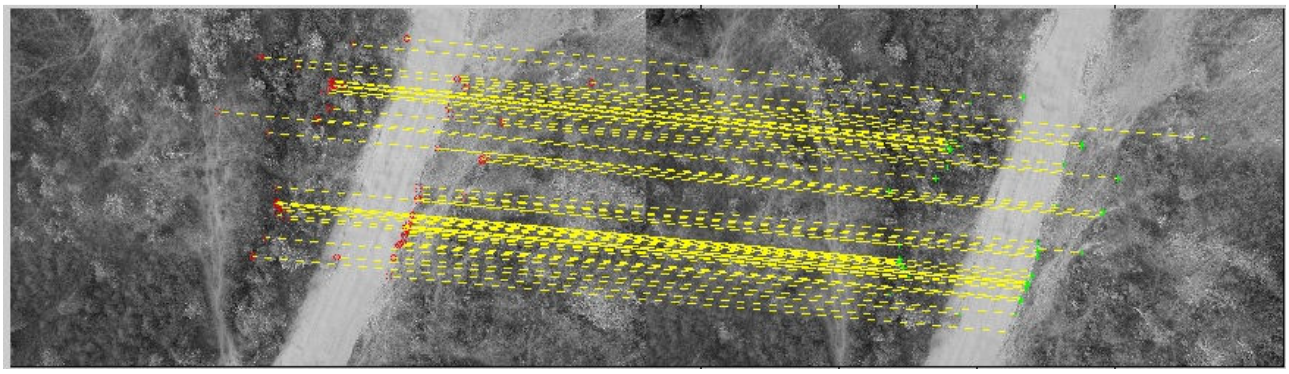

Fig. 8 Conjugate points between two overlap frames

Through the relative orientation stereo model the average camera location error was computed (Table VI). The result from the DLT model and the self-calibration bundle adjustment method to calculate the IOPs and EOPs is shown in Tables VII and VIII respectively.

Fig. 9 shows the image residuals of the camera, which was the outcome result of the camera calibration and ortho-rectification process.

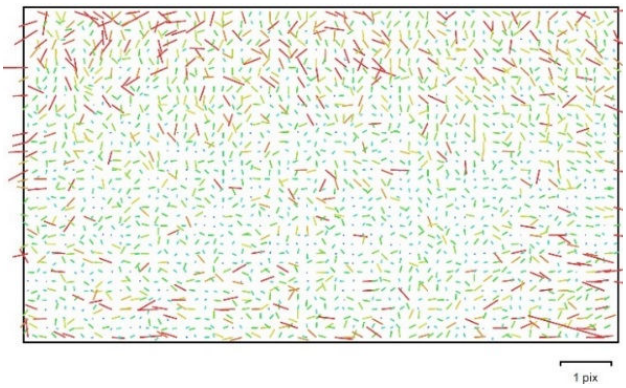

Fig. 9 Image residuals for video frames

The computation for both interior and exterior orientation parameters was done using Agisoft Photoscan software. The computation of absolute orientation is automatic but not autonomous because it involves human interaction where we are prompted to enter the values of the selected ground control points.

A total of 20631 tie points were successfully matched within 78 frames, and the points are evenly spread across the image, which implies, there is no spatial bias in the results. It can also be observed from Fig. 9, that the residuals are randomly distributed in magnitude and direction; this also implies that there is no obvious systematic error in the residuals. The root mean square residual is 0.674679 pix.

TABLE VI
AVERAGE CAMERA LOCATION ERROR

X error (m)	7.087607
Y error (m)	4.113576
Z error (m)	3.460632
Total error	8.895598

TABLE VII
DLT MODEL RESULTS

Row (ω)	-0.0524789
Pitch (ϕ)	0.0042136
Yaw (κ)	-1.037061
u_0	2409.78
v_0	2380.12
f	4634.87

In Table VII, u_0 and v_0 are the coordinates of the principal point. Also the lens distortion is not considered here, this is because the DLT method does not give very accurate results, and hence, the solved IOPs and EOPs will be used as initial values in (1).

In Table VIII, (K_1, K_2, K_3) represents radial distortion coefficients while (P_1, P_2) represent the tangential distortion coefficients.

After the ortho-rectification process, the ortho-images (corrected frames) are mosaicked together to form a map covering the test area (Fig. 10).

TABLE VIII
SELF-CALIBRATION RESULTS

Row (ω)	-0.0545097
Pitch (ϕ)	0.0087668
Yaw (κ)	-1.0087921
u_0	2420.61
v_0	1335.46
K_1	-0.0310589
K_2	0.0280943
K_3	-0.0188507
P_1	0
P_2	0

In order to georeference the ortho-rectified mosaicked imagery, it was merged with the digital globe and on the basis of the 6 GCPs, the accuracy is between 3 to 5 meters.

Fig. 10 Mosaicked images covering test area

VII. CONCLUSION

Our four-step ortho-rectification approach for time critical events has proven successful for a number of reasons. Firstly, our method for ortho-rectification although, is not autonomous, it does not require significant operator interaction. Also, the error assessment during the matching of conjugates on frames shows that the image RMS residual value (0.674679 pix) is sufficient to pin point targets locations in a video scene. The video camera was able to produce frames of forward overlap of 75% and side overlap of 40%, this improves automatic tie point collection. Moreover, cost and turnaround time for production of ortho-rectified mosaics are quite small when compared with the traditional method. This is so, because less time and money are spent on ground control points and tie point collection and the automation of matching these points. However, there is still room for improvement and need for further research.

ACKNOWLEDGMENT

This project was funded by the Tertiary Education Trust Fund (TETFUND). Authors would like to sincerely thank to Sunday Idajili and his flight screw for their support in carrying out the flight missions.

REFERENCES

[1] M. Kontitsis, M., Valavanis, K., N. Tsourveloudis , "A UAV Vision System for Airborne Surveillance," In Proc. of the IEEE International Conference on Robotics and Automation, 2004, pp. 77–83.
[2] D.W. Casbeer, D.B. Kingston, R.W. Bear , T.W. McLain, and S.M. Li, "Cooperative Forest Fire Surveillance Using a Team of Small Unmanned Air Vehicles.", Intl. Journal of System Science, January 2005, pp 1-18.
[3] B.O. Olawale, C.R. Chatwin, R.C.D. Young, P.M. Birch, F.O. Faithpraise and A.O. Olukiran, "Real-Time Monitoring Of Buried Oil Pipeline Right-Of-Way for Third-Party Incursion", International Journal of Innovative Science, Engineering & Technology, Vol. 2 Issue 2,February 2015, pp. 163-173.
[4] B. Colfman, M. McCord, and K. Redmill, "Surface Transportation Surveillance from Unmanned Aerial Vehicles" *Proc. Of the 83rd Annual Meeting of the Transportation Research Board*, 2004.
[5] J. Allen, and B. Walsh, "Enhanced Oil Spill Surveillance, Detection and Monitoring through the Applied Technology of Unmanned Air Systems". In: *Proceedings of the 2008 international oil spill conference.*
[6] R. W. Beard, T. W. McLain, D. B. Nelson, D. Kingston, and D. Johanson, "Decentralized cooperative aerial surveillance using fixed-wing miniature UAVs," Proc. IEEE, July 2006, vol. 94, no. 7, pp. 1306–1323.
[7] Fransaer, D., Vanderhaeghen, F., Everaerts, J., "PEGASUS: Business Plan for a Stratospheric Long Endurance UAV System for Remote Sensing". The International Archives of the Photogrammetry, Remote Sensing and Spatial Information Sciences, Istanbul, Turkey, GITC, Lemmer, Netherlands, 2004.
[8] A. Ollero, J. Ferruz, F. Caballero, S. Hurtado, L. Merino, "Motion Compensation and Object Detection for Autonomous Helicopter Visual Navigation in the Comets System". In: Proc. of the IEEE International Conference on Robotics and Automation, 2004, pp. 19–24.
[9] Anon, "*Functional Specification for a Satellite Surveillance System*", Andrew Palmer and Associates Report NR01003, March 2001.
[10] . M.D.F Bento, "Unmanned Aerial Vehicles: An Overview. *Inside GNSS "*, February, 2008, pp. 54-61.
[11] N. Mohamed, I. Jawhar, "A Fault-Tolerant Wired/Wireless Sensor Network Architecture or Monitoring Pipeline Infrastructures", in Proc. Int. Conference on Sensor Technologies and Applications (SENSORCOMM 2008), Cap Esterel, France,25–31 August 2008; pp. 179-184.
[12] Y. DU, P.M. Teillet, and J.Cihlar, "Radiometric Normalization of Multi-Temporal High-Resolution Satellite Images with Quality Control for Land Cover Change Detection: Remote Sensing of Environment", 2002, pp. 123–134,
[13] S. Chen, B. Mulgrew, and P. M. Grant, "A Clustering Technique for Digital Communications Channel Equalization Using Radial Basis Function Networks," *WASET Trans. Neural Networks*, vol. 4, pp. 570–578, July 1993.
[14] B. Horn *Robot Vision*, MIT Press, 1986, pp 314 – 315.
[15] K. Kobayashi, C. Mori, "Relations between the Coefficients in the Projective Transformation Equations and the Orientation Element of the Photograph". Journal of Photogrammetric Engineering and Remote Sensing. Vol. 63, No. 9, September 1997, pp.1121-1127.
[16] Z. Li, J. Chen, and E. Baltsavias. Advances in Photogrammetry, Remote Sensing and Spatial Information Sciences, 2008 ISPRS Congress Book. CRC Press, Taylor & Francis Group, Boca Raton, London, New York, Leiden, p. 527.
[17] E.M Mikhail, J.S. Bethel, J.C. McGlone. Introduction to Modern Photogrammetry. John Wiley & Sons Inc., New.
[18] http://www.dji.com/product/spreading-wings-s800/spec (Accessed: 11 July 2013).
[19] Z. Guoqing, ''Near Real-Time Orthorectification and Mosaic of Small UAV Video Flow for Time-Critical Event Response' 'in Proc. o Geoscience and Remote Sensing, IEEE, 47(3), March 2009.
[20] Y. I. Abdel-Aziz and H. M. Karara, "Direct Linear Transformation from Comparator Coordinates into Object Space Coordinates in Close-Range Photogrammetry," in Proc. Symp. Close-Range Photogrammetry, Falls Church, VA, 1971, pp. 1–18, Amer. Soc. of Photogrammetry.
[21] J. Skaloud, M. Cramer, and K. P. Schwarz, "Exterior Orientation by Direct Measurement of Camera and Position," in Proc. Int. Archives Photogrammetry Remote Sens., Vienna, Austria, 1996, vol. XXXI, pp. 125-130, Part B3.
[22] Gomarasca, Mario A. *Basics of Geomatics*. Dordrecht: Springer, 2009. Print.

Babatunde Olawale is a current doctoral post graduate student at the University of Sussex, United Kingdom. He had his first degree in (B.Tech) Computer Engineering in the year 2000. He has three different post graduate degrees in the following fields – Master in information Technology in the year 2005, Master in Computer Science in the year 2007 and Master in Security Systems and Technology in the year 2011.

He is a lecturer at the Osun state polytechnic, Nigeria since 2001 to date. His research areas are: image processing, remote sensing, computer vision and photogrammetry.

Chris. R. Chatwin holds the Chair of Engineering, University of Sussex, UK; where, *inter alia*, he is Research Director of the "iisp Research Centre." and the Laser and Photonics Systems Engineering Group. At Sussex has been a member of the University: Senate, Council and Court.

He has published two research monographs: one on numerical methods, the other on hybrid optical/digital computing - and more than two hundred international papers. Professor Chatwin is on the editorial board of the International Journal "Lasers in Engineering".

He is also a member of: the Institution of Electrical and Electronic Engineers; IEEE Computer Society; the British Computer Society; the Association of Industrial Laser Users, European Optical Society. He is a Chartered Engineer, Euro-Engineer, International Professional Engineer, Chartered Physicist, Chartered Scientist and a Fellow of: The Institution of Electrical Engineers, The Institution of Mechanical Engineers, The Institute of Physics and The Royal Society for Arts, Manufacture and Commerce

Rupert Young is a reader at the Department of Engineering and Design, University of Sussex United Kingdom. He graduated from Glasgow University where he gained his PhD in Coherent Optical Signal Processing.

He is a member of the Society of Photo-optical and Instrumentation Engineers. He is also a member of Optical Society of America.

His present research areas are Computer Vision & Image Processing - Pattern Recognition, Computer Vision and Image Processing - Security, Genetic Algorithms (CS), Holography Instrumentation, Medical Informatics, and Photonics

Phil Birch completed his PhD at the University of Durham in 1999 on Liquid Crystal Devices in Adaptive Optics. The systems built used various liquid crystal spatial light modulators (SLMs) to correct for phase aberrations introduced by atmospheric turbulence. This is important for astronomical imaging and free space optical communications.

He has worked in industry developing rapid prototyping equipment and optical metrology systems. Since working at the University of Sussex he has been researching COMPUTER generated holograms (CGH), correlation pattern matching, and optical microscopy. He has also worked with industrial partners in image processing, object detection and tracking.

Fina O. Faithpraise obtained her first degree in computer science and Engineering at Enugu State University of Science and Technology, Nigeria. She obtained a Master of Science degree in engineering physics from the University of Calabar, Cross River State, Nigeria. She had doctoral degree at the University of Sussex, Brighton, United Kingdom.

She is currently a lecturer at the University of Calabar, Nigeria. Her research areas are: image processing, computer security and biomedical imaging.

Adunni. O. Olukiran is a current doctoral post graduate student at Ladoke Akintola University of Technology, Ogbomoso, Oyo State, Nigeria, where she also had her first degree in Computer Engineering in 2010. She had her master degree in Computer and Network Security at Middlesex University London, United Kingdom.

She is currently, a lecturer at Osun State Polytechnic, Iree, Nigeria. Her research areas are: Computer security, network security cryptography.